Spin Hall Effect of Light in a Random Medium

Tamara Bardon-Brun, Dominique Delande, Nicolas Cherroret

Spin Hall Effect of Light in a Random Medium

Tamara Bardon-brun, Dominique Delande, and Nicolas Cherroret*
Laboratoire Kastler Brossel, Sorbonne Université, CNRS, ENS-PSL University, Collège de France; 4 Place Jussieu, 75005 Paris, France

(Received 13 March 2019; revised manuscript received 22 May 2019; published 23 July 2019)

We show that optical beams propagating in transversally disordered materials exhibit a spin Hall effect and a spin-to-orbital conversion of angular momentum as they deviate from paraxiality. We theoretically describe these phenomena on the basis of the microscopic statistical approach to light propagation in random media, and show that they can be detected via polarimetric measurements under realistic experimental conditions.

DOI: 10.1103/PhysRevLett.123.043901

In random media, exploiting of the common wavelike nature of photons and electrons has led to the observation of several optical analogues of condensed-matter phenomena. Well-known examples include fluctuations of photon conductance [1], weak localization of light [2,3], or optical Anderson insulators [4,5]. In Faraday active materials, transverse diffusive currents resembling the Hall effect were also predicted [6] and observed [7], and characterizations of photon localization under partially broken time-reversal symmetry were reported [8,9], in analogy with charged electrons in magnetic fields [10]. Recently, the propagation of paraxial light through disordered arrays of helical waveguides even made it possible to realize a topological photonic Anderson insulator [11].

A currently open question is whether spin-orbit interactions (SOI) of light, i.e., the coupling between the spatial and polarization degrees of freedom of an optical wave front, can be achieved in a random medium. A positive answer would be appealing, since in solids spin-orbit coupling is known to affect quantum transport, giving rise, e.g., to weak antilocalization, or driving random systems to other symmetry classes [12]. The generation of chiral photons in random environments via SOI could also be used as a tool for wave front shaping techniques [13] or, at a more fundamental level, as a new way to design topological insulators [14,15]. A particularly interesting manifestation of SOI is the optical spin Hall effect (SHE), which refers to helicity dependent subwavelength shifts of the trajectory of circularly polarized beams, in analogy with their electronic counterparts [16]. Originally identified for light refracted or reflected at interfaces (Imbert-Fedorov effect) [17,18] and later in gradient-index materials (optical Magnus effect) [19,20], the SHE of light was recently described at a general level on the basis of a geometric Berry phase [21,22]. On the experimental side, pioneering measurements at interfaces were carried out in optics [23] and plasmonics [24], and nowadays SOI of light have become a promising tool for the generation of vortex beams or the control of nano-optical systems [25,26]. In this Letter, we demonstrate that the SHE of light is generically present in *transversally* disordered media, a geometry recently exploited in the context of wave localization [5,11,27,28]. We find that the SHE emerges for beams tilted with respect to the optical axis. The effect is robust vs disorder averaging and controllable via the beam's angle of incidence, i.e., the transverse wavelength, unlike conventional shifts at interfaces which are governed by the optical wavelength. While, close to paraxiality, the SHE is small, we show that it can be strongly magnified and detected via polarimetric measurements under realistic experimental conditions.

In an inhomogeneous medium of permittivity distribution $\epsilon(\boldsymbol{r})$, it was shown from semiclassical considerations that the mean coordinate $\mathbf{R}$ and dimensionless wave vector $\mathbf{P} = \boldsymbol{k}c/\omega$ of an optical beam obey $\dot{\mathbf{R}} = \mathbf{P}/P - (\sigma c/\omega P^3)\mathbf{P} \times \dot{\mathbf{P}}$ and $\dot{\mathbf{P}} = \boldsymbol{\nabla}\sqrt{\epsilon(\boldsymbol{R})}$, where σ is the beam helicity, ω the optical frequency, c the vacuum speed of light, and the dot denotes derivation with respect to the optical path length [20–22]. The first equation of motion emphasizes the spin Hall effect of light, a helicity dependent, subwavelength spatial shift of the beam. Suppose now that $\epsilon(\boldsymbol{r})$ describes a random medium. If the latter is statistically *isotropic*, the beam momentum distribution and permittivity gradient are typically uncorrelated so that disorder averaging leads to $\dot{\mathbf{R}} = \mathbf{P}/P$: no shift survives on average [29]. To observe a finite optical SHE, a statistically *anisotropic* disorder should be used. A simple configuration fulfilling this requirement is illustrated in Fig. 1: a monochromatic collimated beam, of wave vector $\boldsymbol{k}$ lying in the (x, z) plane, propagates in a material with disorder only in the plane $\boldsymbol{r}_\perp = (x, y)$: $\epsilon(\boldsymbol{r}) = \epsilon(\boldsymbol{r}_\perp)$. This geometry has been much studied in the framework of the paraxial wave equation, in which the coordinate z plays the role of an effective propagation time [30]. By going beyond the paraxial description, we find that beams carrying a finite helicity are laterally shifted as soon as their transverse wave

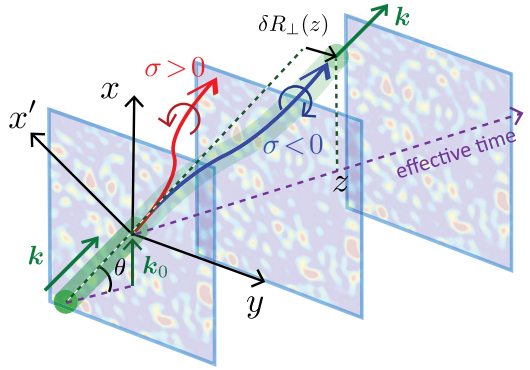

FIG. 1. We consider the propagation of a collimated beam of wave vector $\boldsymbol{k}$ through a medium spatially disordered in the (x, y) plane and homogeneous along the optical axis z. As soon as the transverse wave vector $\boldsymbol{k}_0$ (along the x axis) is nonzero, the disorder-average centroid of the coherent mode is shifted laterally along y as z increases (spin Hall effect). The shift is proportional to the beam helicity σ and shows up even if the medium is statistically homogeneous.

vector $\boldsymbol{k}_0 = k_0\boldsymbol{e}_x$ is nonzero. This shift, which constitutes the optical SHE in a random medium, is visible in the so-called coherent mode, namely, before the beam has been converted into a diffusive halo due to multiple scattering [31]. Specifically, for an incoming beam of complex polarization vector $\boldsymbol{e}(z=0) = (\boldsymbol{e}_{x'} + e^{i\phi}\boldsymbol{e}_y)/\sqrt{2}$, $(\boldsymbol{e}_{x'} \equiv \boldsymbol{e}_y \times \boldsymbol{k}/k)$, we find a lateral shift (see Fig. 1)

$$\delta R_\perp(z) = -\frac{\sigma}{k_0}\left(1 - \frac{1}{\cosh(z/2z_{\mathrm{SH}})}\right) \tag{1}$$

at small angle of incidence $\theta \simeq k_0/k \equiv \hat{k}_0$, with $\sigma = \sin\phi$ the beam helicity, $\sigma = +1$ (-1) for left- (right-)handed circular polarization [32]. The shift continuously increases as the beam propagates deeper in the random medium, until it saturates at $\sim 1/k_0$ beyond a characteristic time $z_{\mathrm{SH}} \equiv z_s/\hat{k}_0^2$, where z_s is the scattering mean free time [33]. The SHE vanishes for linearly polarized light, $\sigma = 0$. Note here the peculiarities of the transverse disorder scheme: the spin Hall shift evolves in time and is on the order of the transverse wavelength $1/k_0$, namely it is much larger than conventional shifts $\propto 1/k$ observed at interfaces [26] and is directly controllable via the angle of incidence.

To demonstrate Eq. (1), we have used a general vector wave treatment based on the exact optical Dyson equation in random media [31,34–36]. Within this framework, we consider the evolution of the coherent mode in a transversally disordered material illuminated at $z = 0$ by a beam of electric field profile $\mathbf{E}(\boldsymbol{r}_\perp, z=0)$. To describe this evolution, we define the normalized intensity, $\hat{I}(\boldsymbol{r}_\perp, z) \equiv I(\boldsymbol{r}_\perp, z)/I_{\mathrm{tot}}(z)$, where $I(\boldsymbol{r}_\perp, z) \equiv |\langle \mathbf{E}(\boldsymbol{r}_\perp, z)\rangle|^2$, $I_{\mathrm{tot}}(z) \equiv \int d^2\boldsymbol{r}_\perp |\langle \mathbf{E}(\boldsymbol{r}_\perp, z)\rangle|^2$ and the brackets refer to disorder averaging. The normalization is here introduced so to work with a conservative quantity, as in a random medium the intensity of the coherent mode decays exponentially beyond z_s [31], an effect we will discuss later on. The components E_j $(j = x, y, z)$ of the complex electric field obey the Helmholtz equation

$$[\Delta\delta_{ij} - \nabla_i\nabla_j + k^2\delta_{ij}(1 + \delta\epsilon(\boldsymbol{r}_\perp)/\bar{\epsilon})]E_j(\boldsymbol{r}_\perp, z) = 0. \tag{2}$$

Disorder is here encoded in random permittivity fluctuations $\delta\epsilon(\boldsymbol{r}_\perp) = \epsilon(\boldsymbol{r}_\perp) - \bar{\epsilon}$ around a mean value $\bar{\epsilon}$. We choose them Gaussian distributed and correlated according to the general form $\overline{\delta\epsilon(\boldsymbol{r}_\perp)\delta\epsilon(\boldsymbol{r}'_\perp)}/\bar{\epsilon}^2 = B(\boldsymbol{r}_\perp - \boldsymbol{r}'_\perp)$, where B is an isotropic decaying function. The disorder average field, $\langle E_i(\boldsymbol{r}_\perp, z)\rangle = \int d^2\boldsymbol{k}_\perp/(2\pi)^2 \langle t_{ij}(\boldsymbol{k}_\perp, z)\rangle E_j(\boldsymbol{k}_\perp, z=0) e^{i\boldsymbol{k}_\perp\cdot\boldsymbol{r}_\perp}$, is governed by the average transmission coefficient of the medium, $\langle t_{ij}(\boldsymbol{k}_\perp, z)\rangle = 2i(k^2 - \boldsymbol{k}_\perp^2)^{1/2}\langle G_{ij}(\boldsymbol{k}_\perp, z)\rangle$, where G_{ij} is the Green's tensor of Eq. (2) [37]. To find its disorder average, we have diagonalized the Dyson equation for its Fourier transform, $\langle \mathbf{G}(\boldsymbol{k}_\perp, k_z)\rangle = [\mathbf{G}^{(0)}(\boldsymbol{k}_\perp, k_z)^{-1} - \boldsymbol{\Sigma}(\boldsymbol{k}_\perp, k_z)]^{-1}$, where $G_{ij}^{(0)}(\boldsymbol{k}_\perp, k_z) = (\delta_{ij} - \hat{k}_i\hat{k}_j)/(k^2 - \boldsymbol{k}_\perp^2 - k_z^2 + i0^+)$ and the self-energy tensor is evaluated at the level of the Born approximation: $\Sigma_{ij}(\boldsymbol{k}_\perp, k_z) = k^4 \int d^2\boldsymbol{k}'_\perp/(2\pi)^2 B(\boldsymbol{k}_\perp - \boldsymbol{k}'_\perp) G_{ij}^{(0)}(\boldsymbol{k}'_\perp, k_z)$ [33]. This calculation is detailed in the Supplemental Material [29]. To make it concrete, we model the incident light by a collimated Gaussian beam $\mathbf{E}(\boldsymbol{r}_\perp, z=0) = \sqrt{2/(\pi w_0^2)}\exp(-r_\perp^2/w_0^2 + i\boldsymbol{k}_0\cdot\boldsymbol{r}_\perp)\boldsymbol{e}(z=0)$ with unit polarization vector $\boldsymbol{e}(z=0) = (\boldsymbol{e}_{x'} + e^{i\phi}\boldsymbol{e}_y)/\sqrt{2}$ and waist w_0 such that $w_0 k_0 \gg 1$. We find

$$\hat{I}(\boldsymbol{r}_\perp, z) = \hat{I}(\boldsymbol{r}_\perp - \boldsymbol{R}_\perp(z), 0). \tag{3}$$

This result describes a shift of the centroid $\boldsymbol{R}_\perp(z) \equiv \int d^2\boldsymbol{r}_\perp \boldsymbol{r}_\perp \hat{I}(\boldsymbol{r}_\perp, z)$ as the beam evolves along the effective time axis z. The shift is

$$\boldsymbol{R}_\perp(z) = \hat{\boldsymbol{k}}_0 z + \delta R_\perp(z)\boldsymbol{e}_y. \tag{4}$$

In Eq. (4), the first term on the right-hand side is the usual geometrical-optics contribution, while the second term is the spin Hall shift, with $\delta R_\perp(z)$ given by Eq. (1) at leading order in $\hat{k}_0 \ll 1$ [29], and the mean free time follows from the angular average of the disorder power spectrum, $z_s^{-1} = k^3\langle B(k_0, \hat{\boldsymbol{k}}_\perp - \hat{\boldsymbol{k}}'_\perp)\rangle_{\hat{k}'_\perp}/4$ [38]. The left panel in Fig. 2 shows $\delta R_\perp(z)$ vs z in units of $\lambda = 2\pi/k$, for three values of $\hat{k}_0$. Its asymptotic limit, $\delta R_\perp(z \gg z_{\mathrm{SH}}) = -\sigma/k_0$, increases with decreasing k_0. Note that unlike the beam centroid, the mean momentum $\boldsymbol{k}$ remains *fixed* during propagation, as the coherent mode by definition describes the unscattered part of the optical signal.

Often, optical SHE are associated with a conversion of angular optical momentum: the spin angular momentum of the beam (characterizing its mean polarization) is converted into an orbital angular momentum (characterizing its

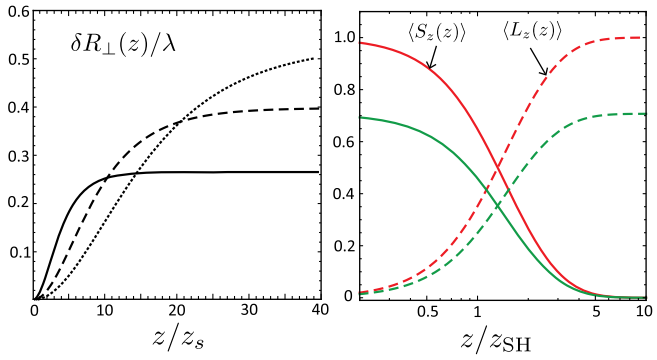

FIG. 2. Left: spin Hall shift vs z/z_s (z_s mean free time) of a right-handed circularly polarized beam, for $\hat{k}_0 = 0.3$, 0.4, and 0.6 from top to bottom. Right: spin-to-orbital angular momentum conversion. As z increases, the z component of the spin angular momentum $\langle S_z(z)\rangle$ (solid curves) decreases and the beam acquires a finite orbital angular momentum $\langle L_z(z)\rangle$ (dashed curves), with the sum $\langle S_z(z)\rangle + \langle L_z(z)\rangle = \sigma$ conserved. Upper and lower curves correspond to $\sigma = 1$ and 0.7, respectively.

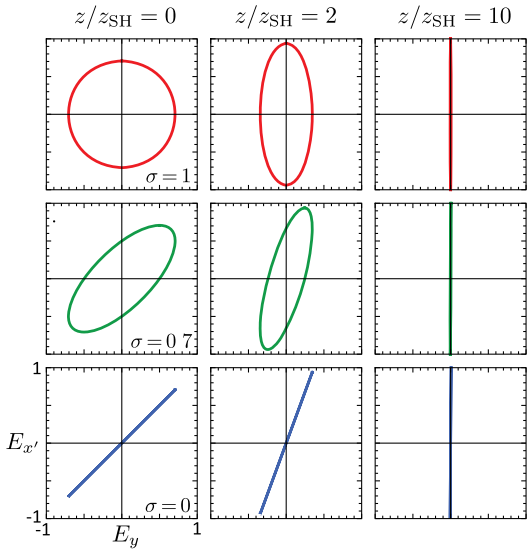

FIG. 3. Evolution of the polarization in the plane (x', y) at increasing z, for $\sigma = 1$ (top panels, initial circular polarization), 0.7 (middle panels, elliptic polarization), and 0 (lower panels, linear polarization). Whatever the initial polarization, the beam always end up linearly polarized along x' when $z \gg z_{\rm SH}$.

mean spatial structure) [26]. It turns out that, in a random medium, this picture holds for the coherent mode as well. To show this, we have computed the angular momentum of the coherent mode, using the statistical approach described above. At small $\hat{k}_0$, the latter decomposes into an orbital contribution, $\langle \mathbf{L}(z)\rangle \equiv -i\int d^2\boldsymbol{r}_\perp \langle E_i^*(\boldsymbol{r}_\perp, z)\rangle (\boldsymbol{r}\times\nabla)\langle E_i(\boldsymbol{r}_\perp, z)\rangle / I_{\rm tot}(z)$, and a spin contribution, $\langle \mathbf{S}(z)\rangle \equiv -i\int d^2\boldsymbol{r}_\perp \langle \mathbf{E}^*(\boldsymbol{r}_\perp, z)\rangle \times \langle \mathbf{E}(\boldsymbol{r}_\perp, z)\rangle / I_{\rm tot}(z)$ [39]. From the solution of the Dyson equation, we derive the transparent relation $\langle \mathbf{L}(z)\rangle = \delta\boldsymbol{R}_\perp(z)\times\boldsymbol{k}$ [29], which shows that the SHE can be regarded as the emergence of a finite orbital momentum. Of peculiar interest are the axial components $\langle L_z(z)\rangle$ and $\langle S_z(z)\rangle$, which explicitly read

$$\langle L_z(z)\rangle = \sigma\left[1 - \frac{1}{\cosh(z/2z_{\rm SH})}\right],$$
$$\langle S_z(z)\rangle = \sigma - \langle L_z(z)\rangle. \tag{5}$$

$\langle L_z(z)\rangle$ and $\langle S_z(z)\rangle$ are displayed in the right panel of Fig. 2 as a function of z. As z increases, the SOI mediated by the disorder convert $\langle S_z\rangle$ into $\langle L_z\rangle$ with no net angular momentum transferred to the medium, which only acts as an intermediary. Note that unlike conversions previously reported in inhomogeneous anisotropic materials (q plates) [40], here the spatial beam shape is preserved, see Eq. (3), so that the orbital angular momentum is associated with a global beam torsion and not with a vortex. In our system, the exact conservation of $\langle L_z(z)\rangle + \langle S_z(z)\rangle = \sigma$ stems from the statistical rotational symmetry around the z axis. The spin-to-orbital conversion described here also indicates that the mean polarization of the incoming beam is not fixed, but evolves during propagation. From the Fourier component $\langle \mathbf{E}(\boldsymbol{k}_\perp \simeq \boldsymbol{k}_0, z)\rangle \propto \boldsymbol{e}(z)$, we extract the explicit expression of the mean polarization vector $\boldsymbol{e}(z)$. For an initial beam with $\boldsymbol{e}(z=0) = (\boldsymbol{e}_{x'} + e^{i\phi}\boldsymbol{e}_y)/\sqrt{2}$, we find [29]

$$\boldsymbol{e}(z) = \frac{\boldsymbol{e}_{x'} + e^{i\phi}\exp(-z/2z_{\rm SH})\boldsymbol{e}_y}{\sqrt{1+\exp(-z/z_{\rm SH})}}. \tag{6}$$

Trajectories of the polarization in the plane (x', y) pertained to Eq. (6) are represented in Fig. 3 at increasing values of z for $\sigma = 1$, 0.7, and 0 (circular, elliptic, and linear polarization, respectively). Because of the angular momentum conversion, the beam always end up linearly polarized along x' beyond the spin Hall time $z_{\rm SH}$, whatever the initial polarization. Interestingly, the polarization vector of initially linearly polarized light rotates as well, although no SHE arises in this case.

We finally present an experimental proposal for measuring the optical SHE in a random medium. As seen from Eq. (1), the maximum shift $\sim 1/k_0$ is reached at times $z > z_{\rm SH} = z_s/\hat{k}_0^2$. Since the coherent mode gets attenuated at $z > z_s$ because of photon scattering, observing the SHE requires either to decrease $z_{\rm SH}$ by deviating more from paraxiality or to *magnify* the shift. We now show that this second option can be readily achieved by means of a polarimetric measurement, in the spirit of recent works on shifts at interfaces [23,24]. The strategy is based on a technique analogous to weak measurements in quantum mechanics [41,42]. To illustrate it, we suppose that the incoming beam is linearly polarized along x', $\boldsymbol{e}(z=0) = \boldsymbol{e}_{x'}$. In this configuration, the mean polarization $\boldsymbol{e}(z)$ remains fixed, but its polarization distribution,

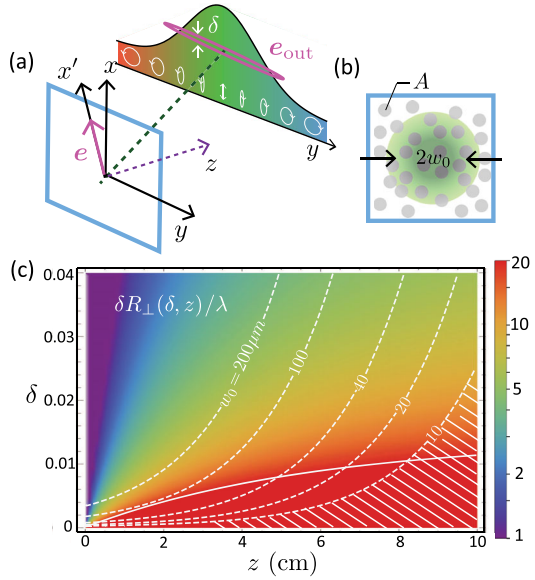

FIG. 4. (a) When propagating in disorder, beams polarized along $\boldsymbol{e}_{x'}$ acquire an inhomogeneous polarization structure with circularly polarized wings. By detecting light along $\boldsymbol{e}_{\rm out} \propto (\boldsymbol{e}_y + i\delta\boldsymbol{e}_{x'})$ with $\delta \ll 1$, one magnifies the spin Hall shift. (b) To estimate the mean free time z_s, we consider a random array of guides of section A, surface density ρ, and relative refractive index $\delta n/n$. Taking $\lambda = 532$ nm, $\delta n/n = 7\times10^{-4}$, $n = 1.5$, $\hat{k}_0 = 0.57$, $A = 20\ \mu\text{m}^2$, and $\rho = 0.02\ \mu\text{m}^{-2}$, we find $z_s \simeq 1$ cm. (c) Density plot of the spin Hall shift in wavelength units, Eq. (7), vs z and δ. Dashed white curves indicate the boundary where the constraint (8) becomes an equality for various beam waists w_0. The SHE is detectable in the region lying above these curves. The solid curve indicates the level set $\delta R_\perp = 20\lambda$.

$\propto \langle \mathbf{E}^*(\boldsymbol{r}_\perp,z)\rangle \times \langle \mathbf{E}(\boldsymbol{r}_\perp,z)\rangle \propto \mathbf{e}_{x'} \times \boldsymbol{r}_\perp \exp(-2r_\perp^2/w_0^2)$, is inhomogeneous: the core of the beam is linearly polarized while the wings $|\boldsymbol{r}_\perp| \sim w_0$ are circularly polarized with opposite helicities, as illustrated in Fig. 4(a). Thus, by detecting light along the polarization $\boldsymbol{e}_{\rm out} = (\boldsymbol{e}_y + i\delta\boldsymbol{e}_{x'})/\sqrt{1+\delta^2}$, with δ a small real number, one will measure a shift on the order of w_0. Precisely, we find a beam centroid, now defined as $\boldsymbol{R}_\perp = \int d^2\boldsymbol{r}_\perp \boldsymbol{r}_\perp |\langle \mathbf{e}^*_{\rm out}\cdot \mathbf{E}(\boldsymbol{r}_\perp,z)\rangle|^2 / \int d^2\boldsymbol{r}_\perp |\langle \boldsymbol{e}^*_{\rm out}\cdot \mathbf{E}(\boldsymbol{r}_\perp,z)\rangle|^2$ [29]:

$$\delta R_\perp(\delta,z) = -\frac{\delta}{k_0}\frac{1-\exp(-z/2z_{\rm SH})}{\delta^2 + [1-\exp(-z/2z_{\rm SH})]^2/(w_0k_0)^2}. \tag{7}$$

Compared to the case where no polarimetric measurement is performed, Eq. (1), the SHE can now be enhanced by several orders of magnitude by tuning δ, with a maximum value $\delta R_\perp \sim w_0$ for $z \gg z_{\rm SH}$ and $\delta \simeq 1/w_0k_0$ [24]. To establish the practical conditions under which the SHE can be measured though, we must additionally account for the attenuation of the coherent mode. This attenuation is both due to the polarimetric measurement, which only selects a fraction δ^2 of the intensity and, as discussed above, to multiple scattering. The latter depletes exponentially the coherent mode, which becomes weaker than the diffusive signal emerging when $z \gg z_s$. This phenomenon imposes constraints on z and δ. To find them, we compare the intensity per unit surface of the coherent mode, $I \simeq 2\delta^2/(\pi w_0^2)\exp(-z/z_s)$ with the diffusive signal I_d. The latter was computed in Ref. [33] in the geometry of transverse disorder: $I_d \simeq [1-\exp(-z/z_p)]/(8\pi Dz)$, where $z_p = 8z_s/5\hat{k}_0^4$ and the diffusion coefficient $D = \hat{k}_0^2 z_s/2$. The constraint $I > I_d$ then reads

$$\frac{w_0^2}{zz_s}[1-\exp(-z/z_p)] < 8\hat{k}_0^2\delta^2\exp(-z/z_s). \tag{8}$$

From this criterion, it appears that the beam waist w_0 should be as small as possible. For a realistic estimation, we consider a medium consisting of a random array of uniformly distributed guides of surface density ρ, relative refractive index $\delta n/n$, and Gaussian profile of section A, $B(\boldsymbol{k}_\perp) = \rho(A\delta n/n)^2\exp(-\boldsymbol{k}_\perp^2 A/4\pi)$, a type of disorder easy to imprint on glass [43,44] [Fig. 4(b)]. With this model we find the mean free time from the Born approximation: $z_s^{-1} = \rho k^2(\delta n/n)^2 A^{3/2}/4\hat{k}_0$. Using this expression, we show in Fig. 4(c) a density plot of the spin Hall shift vs (z,δ), Eq. (7), obtained for $z_s \simeq 1$ cm. For a given waist w_0, the range of parameters where the inequality (8) is satisfied lies above the dashed curve, as explicitly indicated by the shaded area for $w_0 = 10\ \mu$m. This analysis suggests that for $\delta \sim 10^{-2}$, a shift on the order of 20λ (level set indicated by the solid curve) could be detected for $w_0 \sim 10$–$40\ \mu$m.

We have demonstrated the SHE of electromagnetic waves in transverse disorder using the general statistical treatment of wave propagation in random media. We have also proposed a practical experimental configuration where the SHE can be magnified and detected via polarimetric measurements. Even without such a setup, SOI are naturally enhanced as one deviates from paraxiality. While we have focused on the coherent mode, we anticipate that the SHE should show up in the multiple scattering signal as well. Indeed, the coherent mode and scattered intensity are related by the constraint of flux conservation (Ward identity) [31,33]. This implies that SOI are likely, e.g., to shift the diffusive halo and modify mesoscopic phenomena like weak localization [45]. At strong disorder, when the mean free path is on the order of the spin Hall shift $1/k_0$, we also expect Anderson localization to be affected, via a change of the localization length or the emergence of an Anderson transition in 2D, like for electrons [12] or atoms [46]. In practice, the SHE of light in random media could be also exploited with a magnetic field breaking time-reversal invariance to achieve, e.g., topological insulators. As a general consequence of the coupling between polarization and spatial degrees of freedom in an anisotropic

random medium, the SHE of light might be more the rule than the exception, and in particular arise for other material's anisotropies and other types of vector waves.

N. C. thanks Cyriaque Genet and Matthieu Bellec for useful advice and comments.

*cherroret@lkb.upmc.fr

[1] F. Scheffold and G. Maret, Phys. Rev. Lett. **81**, 5800 (1998).
[2] M. P. Van Albada and A. Lagendijk, Phys. Rev. Lett. **55**, 2692 (1985).
[3] P. E. Wolf and G. Maret, Phys. Rev. Lett. **55**, 2696 (1985).
[4] M. V. Berry and S. Klein, Eur. J. Phys. **18**, 222 (1997).
[5] T. Schwartz, G. Bartal, S. Fishman, and M. Segev, Nature (London) **446**, 52 (2007).
[6] B. A. van Tiggelen, Phys. Rev. Lett. **75**, 422 (1995).
[7] G. L. J. A. Rikken and B. A. van Tiggelen, Nature (London) **381**, 54 (1996).
[8] Y. Bromberg, B. Redding, S. M. Popoff, and H. Cao, Phys. Rev. A **93**, 023826 (2016).
[9] L. Schertel, O. Irtenkauf, C. M. Aegerter, G. Maret, and G. J. Aubry, arXiv:1812.06447.
[10] C. W. J. Beenakker, Rev. Mod. Phys. **69**, 731 (1997).
[11] S. Stützer, Y. Plotnik, Y. Lumer, P. Titum, N. H. Lindner, M. Segev, M. C. Rechtsman, and A. Szameit, Nature (London) **560**, 461 (2018).
[12] F. Evers and A. D. Mirlin, Rev. Mod. Phys. **80**, 1355 (2008).
[13] S. Rotter and S. Gigan, Rev. Mod. Phys. **89**, 015005 (2017).
[14] L. Lu, J. D. Joannopoulos, and M. Soljačić, Nat. Photonics **8**, 821 (2014).
[15] T. Ozawa, H. M. Price, A. Amo, N. Goldman, M. Hafezi, L. Lu, M. C. Rechtsman, D. Schuster, J. Simon, O. Zilberberg, and I. Carusotto, Rev. Mod. Phys. **91**, 015006 (2019).
[16] J. Sinova, S. O. Valenzuela, J. Wunderlich, C. H. Back, and T. Jungwirth, Rev. Mod. Phys. **87**, 1213 (2015).
[17] F. I. Fedorov, Dokl. Akad. Nauk SSSR **105**, 465 (1955).
[18] C. Imbert, Phys. Rev. D **5**, 787 (1972).
[19] A. V. Dooghin, N. D. Kundikova, V. S. Liberman, and B. Y. Zel'dovich, Phys. Rev. A **45**, 8204 (1992).
[20] V. S. Liberman and B. Y. Zel'dovich, Phys. Rev. A **46**, 5199 (1992).
[21] K. Yu. Bliokh and Y. P. Bliokh, Phys. Lett. A **333**, 181 (2004).
[22] M. Onoda, S. Murakami, and N. Nagaosa, Phys. Rev. Lett. **93**, 083901 (2004).
[23] O. Hosten and P. Kwiat, Science **319**, 787 (2008).
[24] Y. Gorodetski, K. Y. Bliokh, B. Stein, C. Genet, N. Shitrit, V. Kleiner, E. Hasman, and T. W. Ebbesen, Phys. Rev. Lett. **109**, 013901 (2012).
[25] F. Cardano and L. Marrucci, Nat. Photonics **9**, 776 (2015).
[26] K. Y. Bliokh, F. J. Rodríguez-Fortuño, F. Nori, and A. V. Zayats, Nat. Photonics **9**, 796 (2015).
[27] M. Boguslawski, S. Brake, D. Leykam, A. S. Desyatnikov, and C. Denz, Sci. Rep. **7**, 10439 (2017).
[28] M Boguslawski, S. Brake, J. Armijo, F. Diebel, P. Rose, and C. Denz, Opt. Express **21**, 31713 (2013).
[29] See Supplemental Material at http://link.aps.org/supplemental/10.1103/PhysRevLett.123.043901 for the derivation of Eqs. (1), (3), (4), (6), and (7).
[30] H. De Raedt, Ad Lagendijk, and P. de Vries, Phys. Rev. Lett. **62**, 47 (1989).
[31] P. Sheng, *Introduction to Wave Scattering, Localization, and Mesoscopic Phenomena* (Academic Press, San Diego, 1995).
[32] This expression does not include the constant Imbert-Fedorov shift possibly arising at the interface between the outside and the random medium.
[33] N. Cherroret, Phys. Rev. A **98**, 013805 (2018).
[34] M. J. Stephen and G. Cwillich, Phys. Rev. B **34**, 7564 (1986).
[35] A. Lagendijk and B. A. van Tiggelen, Phys. Rep. **270**, 143 (1996).
[36] A. Lubatsch, J. Kroha, and K. Busch, Phys. Rev. B **71**, 184201 (2005).
[37] R. Berkovits and S. Feng, Phys. Rep. **238**, 135 (1994).
[38] We here neglect the real part of the self-energy, which shifts the average refractive index. We have checked than in usual transversally disordered media, in particular for the model in Fig. 4(b), this real part negligibly contributes to $\delta R_{\perp}(z)$.
[39] K. Y. Bliokh, A. Aiello, and M. A. Alonso, in *The Angular Momentum of Light*, edited by D. L. Andrews and M. Babiker (Cambridge University Press, Cambridge, England, 2012), p. 174.
[40] L. Marrucci, C. Manzo, and D. Paparo, Phys. Rev. Lett. **96**, 163905 (2006).
[41] Y. Aharonov, D. Z. Albert, and L. Vaidman, Phys. Rev. Lett. **60**, 1351 (1988).
[42] I. M. Duck, P. M. Stevenson, and E. C. G. Sudarshan, Phys. Rev. D **40**, 2112 (1989).
[43] M. Bellec, P. Panagiotopoulos, D. G. Papazoglou, N. K. Efremidis, A. Couairon, and S. Tzortzakis, Phys. Rev. Lett. **109**, 113905 (2012).
[44] M. Bellec, C. Michel, H. Zhang, S. Tzortzakis, and P. Delplace, Eur. Phys. Lett. **119**, 14003 (2017).
[45] S. Hikami, A. Larkin, and Y. Nagaoka, Prog. Theor. Phys. **63**, 707 (1980).
[46] G. Orso, Phys. Rev. Lett. **118**, 105301 (2017).